J. Mod. Power Syst. Clean Energy (2016) 4(1):103–112
DOI 10.1007/s40565-015-0180-5

Global synchronous discontinuous pulse width modulation method with fast calculation capability for distributed three-phase inverters

Tao XU[1], Ran WEI[2], Ke ZHOU[2], Feng GAO[1]

Abstract When multiple distributed converters are integrated, the high frequency harmonics will randomly accumulate at the point of common coupling (PCC). This paper proposes a new fast global synchronous discontinuous pulse width modulation (GSDPWM) method of three-phase inverters to effectively attenuate the high frequency current harmonics at PCC. Firstly, the basic principle and the realization method of GSDPWM for three-phase inverters are explained, which can be employed for different modulation types. Then a fast calculation method, which can equally derive the minimized total harmonic distortion (THD) of total current, is proposed to release the calculation burden. Finally, MATLAB simulations and experimental results are presented to verify the performance of GSDPWM.

CrossCheck date: 14 December 2015

Received: 18 October 2015 / Accepted: 18 December 2015 / Published online: 16 January 2016

✉ Feng GAO
fgao@sdu.edu.cn

Tao XU
xutaojason@163.com

Ran WEI
weiranshandong@126.com

Ke ZHOU
43980088@126.com

[1] Key Laboratory of Power System Intelligent Dispatch and Control (Shandong University), Ministry of Education, Jinan 250061, China

[2] State Grid Jining Electric Power Supply Company, Jining 272000, China

Keywords Global synchronous pulse width modulation, Three-phase inverters, High frequency harmonics, Discontinuous pulse width modulation

1 Introduction

Distributed inverters have been widely implemented in many applications, such as photovoltaic (PV) plant, wind plant and microgrid, to connect distributed sources to the power grid [1–5], where distributed inverters are generally controlled by pulse width modulation (PWM) methods. For three-phase inverters, sinusoidal pulse width modulation (SPWM) with the triplen harmonic added and the space vector pulse width modulation (SVPWM) can effectively increase the maximum modulation index to 1.15 [6–8]. Compared with SPWM, the discontinuous pulse width modulation (DPWM) can clamp the associated phase to the positive or negative DC rail, and then significantly reduce the switching losses [9–13]. But DPWM will introduce more high frequency harmonics than SPWM. Ref. [12] presented that when DPWM and SPWM produce the same switching losses by increasing the switching frequency of DPWM, the total harmonic distortion (THD) of DPWM is still larger than that of SPWM when the modulation index is low.

To reduce the high frequency harmonics, LC, LCL or other high order filters can be employed [14–16]. However, LC or LCL resonance peak will decline the inverter performance. Active or passive damping method can be employed to eliminate the resonance peak. But these methods will increase the complexity of the control system. What's more, the high order filter may bring serious resonance problems when many distributed inverters are connected to PCC [17]. Alternatively, the interleaved PWM can reduce the high frequency harmonics [18]. But it cannot be directly applied to multiple

distributed inverters because they are not connected in parallel at the DC side.

Reference [19] proposed the global synchronous pulse width modulation (GSPWM) method, where global synchronous unit (GSU) was employed to realize the basic functions of GSPWM and the high frequency harmonics can be eliminated at PCC. Ref. [20] proposed the method to reduce the switching frequency and the filter size when using GSPWM. When calculating the harmonics of inverters controlled by DPWM, GSPWM will cost much time to calculate the harmonics of discontinuous modulation waveforms. And it is hard to implement these complicated calculations in digital signal processor (DSP) or other digital controllers. Besides, the conventional GSPWM method adopts a particle swarm optimization (PSO) method with many particles and iteration steps to find the optimal phase shift angles and the synchronization frequency. Together with the harmonic calculation procedure, it will definitely increase the operation burden of GSU.

This paper therefore proposes a new method to fast calculate the high frequency harmonics of three-phase inverters when the modulation waveforms are discontinuous. Then, a new processing method to fast calculate the important optimal phase shift angles and the frequency of sending synchronization signals is introduced. Finally, MATLAB simulations and experimental results verify the performance of the proposed method.

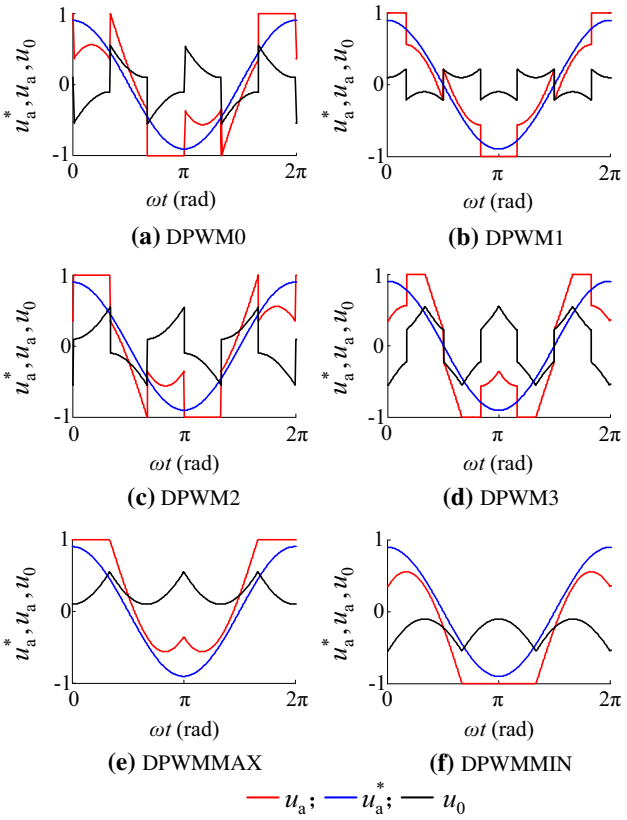

Fig. 1 DPWM modulation waveforms of phase a when $D = 0.9$

2 Basic principle of three-phase PWM

For the three-phase three-wire inverters, any zero-sequence signal can be injected into the modulation [9]. There are 6 kinds of DPWMs generated by adopting different zero-sequence components, which are DPWM0, DWPM1, DPWM2, DPWM3, DPWMMIN, and DPWMMAX [9, 10, 13]. In general, the modulation reference values can be listed as

$$u_s^* = u_s + u_0 \quad s = \text{a,b,c} \tag{1}$$

$$u_a = D\sin(\omega t) \tag{2}$$

where u_s is the modulation reference value of SPWM; u_s^* the modulation reference value of DPWM; u_0 the zero-sequence component; and D the modulation index.

Figure 1 shows the normalized waveforms of u_a, u_a^*, u_0 for 6 kinds of DPWM methods when $D = 0.9$. The main difference among these DPWM methods is u_0 [9, 10].

In addition, the modulation waveform of triplen harmonic PWM consists of both fundamental component and a third-harmonic component [12, 13] as shown in Fig. 2. Given that the modulation waveforms of these modulation methods are discontinuous or non-sinusoidal, the piecewise integration can be employed to calculate the high frequency harmonics [13]. And the only difference is the outer and inner double Fourier integral limits. So DPWMMIN is taken as an example in the following analysis and verification.

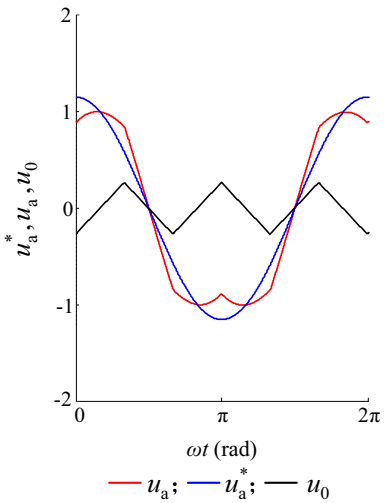

Fig. 2 Modulation waveforms of phase a for the triplen harmonic PWM

3 Principles and realization of global synchronous discontinuous pulse width modulation (GSDPWM)

When three-phase inverters are connected in parallel, the THD of total current will change periodically as same as that analyzed in [19]. For simplicity, this subsection takes two identical three-phase inverters as an example for analysis, and their parameters are listed in Table 1. MATLAB is used to simulate this phenomenon. Assuming the frequency of these two inverters are 10.0001 kHz and 9.9999 kHz due to the unavoidably variable oscillation frequency of crystal inside the digital controller and DPWMMIN is employed, Fig. 3 shows the THD trajectories of currents in 5 s. It is obvious that the THD of total current changes with time progresses and the minimal THD only appears once. Therefore, it is superior to fix the THD of total current to be as small as possible during the operation. GSU and the corresponding carrier phase angle adjustment method can be employed to achieve this objective [19], whose basic structure is shown in Fig. 4.

The primary functions of GSU are to:

1) receive parameters and the PWM type of each inverter, and calculate the high frequency harmonics of total current by using the proposed fast calculation method;
2) calculate $\varphi_{\mathrm{PWM}M\mathrm{best}}$ and f_{syn} with the fast intelligent method. Where $\varphi_{\mathrm{PWM}M\mathrm{best}}$ is the optimal phase shift angle and f_{syn} is the sending frequency of synchronous signals.

However, DPWM will produce different harmonic characteristics compared with SPWM. Therefore, next section will discuss the fast calculation methods for realizing the expected synchronous operation of three-phase inverters.

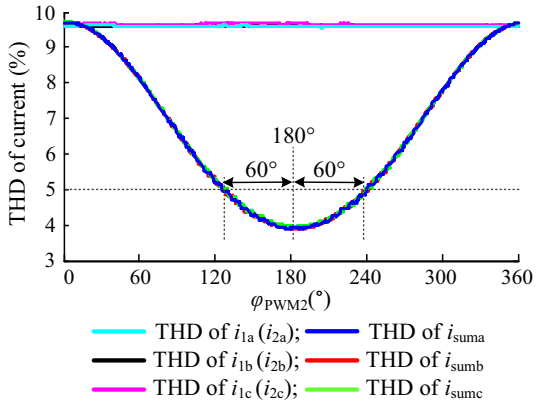

Fig. 3 THD trajectories of the three-phase total currents and output currents of two inverters in 5 s

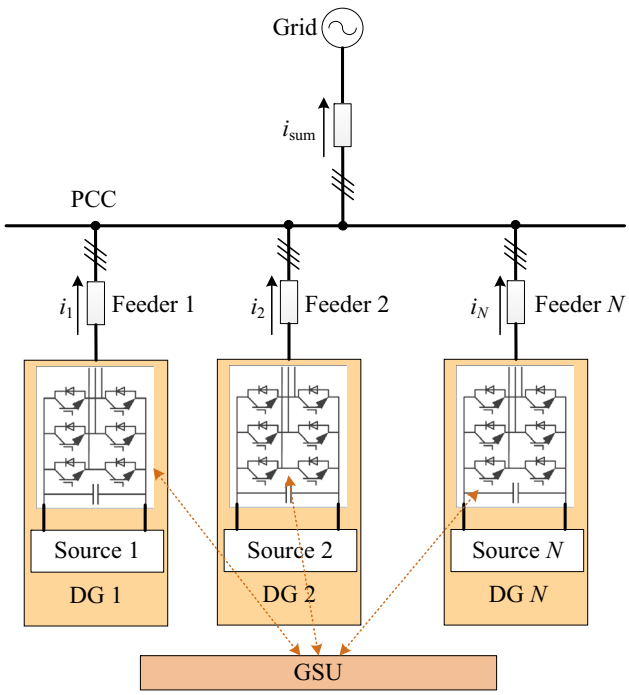

Fig. 4 Basic structure of GSDPWM

4 Fast calculation method of current harmonics

This section proposes a new method to fast calculate the high frequency harmonics of three-phase inverters. A look-up table is developed to help fast calculate the voltage harmonics of each inverter, and then a simplified equivalent harmonic circuit is proposed to calculate current harmonics of the three-phase inverter. Doing so, the total current harmonics can be further derived to get the relationships between total current harmonics and the phase shift angle of each inverter. The current harmonics of three-phase inverter can be analyzed by using the double Fourier method. Assuming u_a*, u_b* and u_c* are symmetrical under steady state, only a few parts of harmonics in u_a* need to be calculated. Specifically, since the phase shift angle of $\varphi_{\mathrm{PWM}M}$ generates the equal effect on three-phase

Table 1 Parameters of two inverters

Inverter	Switchting frequency (kHz)	DC voltage (V)	Filter inductance (mH)	Active power (kW)	DPWM type	Utility grid
1	10.0001	700	5	2.8	DPWMMIN	50 Hz/380 V
2	9.9999	700	5	2.8	DPWMMIN	50 Hz/380 V

currents, it is reasonable to only calculate the current harmonics of one phase. The calculation method of total current harmonics will be presented below.

4.1 Voltage harmonic calculation

Figure 5a shows the general illustration of three-phase inverter M, where u_{Ma}, u_{Mb} and u_{Mc} are the three-phase output voltages; and Z_M refers to the output filter impedance of inverter M. Assuming the grid voltage is purely sinusoidal, the equivalent circuit harmonics can be drawn as Fig. 5b, where u_{hMa}, u_{hMb} and u_{hMc} are the voltage harmonics of u_{Ma}, u_{Mb}, u_{Mc}, respectively.

By using the double Fourier method [13], voltage harmonics can be expressed as:

$$\begin{aligned} u_{hMs} = & \sum_{m=1}^{\infty} \Big[A_{m0}\cos(m(\omega_c t+\varphi_{PWMM})) \\ & + B_{m0}\sin(m(\omega_c t+\varphi_{PWMM}))\Big] \\ & + \sum_{m=1}^{\infty}\sum_{\substack{n=-\infty \\ (n\neq 0)}}^{\infty} \Big[A_{mn}\cos(m(\omega_c t+\varphi_{PWMM}) \\ & + n(\omega_0 t+\theta_s+\theta_0)) + B_{mn}\sin(m(\omega_c t \\ & + \varphi_{PWMM}) + n(\omega_0 t+\theta_s+\theta_0))\Big] \\ & s=a:\theta_s=0;\ s=b:\theta_s=-\tfrac{2\pi}{3};\ s=c:\theta_s=-\tfrac{4\pi}{3} \end{aligned} \tag{3}$$

where m and n are the carrier multiple index and the fundamental multiple index, respectively; A_{m0} and B_{m0} the parameters of carrier multiple harmonics; A_{mn} and B_{mn} the parameters of sideband harmonics.

Compared with SPWM, the modulation reference values of DPWM are discontinuous. So the piecewise integration method is employed here. For DPWMMIN type:

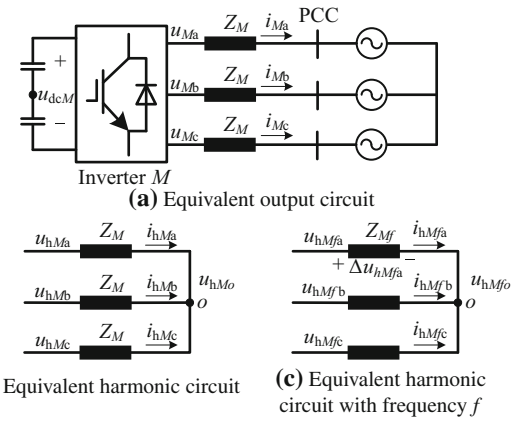

Fig. 5 Illustration of three-phase inverter M

$$A_{mn}+\mathrm{j}B_{mn}=\frac{1}{2\pi^2}\sum_{i=1}^{4}\int_{y_1(i)}^{y_2(i)}\int_{x_1(i)}^{x_2(i)} 2V_{dc}\exp(\mathrm{j}(mx+ny))\mathrm{d}x\mathrm{d}y \tag{4}$$

where i is the number of each piece; $x_1(i)$, $x_2(i)$, $y_1(i)$, and $y_2(i)$ are the inner or outer integral limits which are listed in Table 2.

Equation (3) can also be expressed as

$$u_{hMs}=\sum_{f=f_{1M}+1}^{\infty} u_{hMfs} \quad s=a,b,c \tag{5}$$

u_{hMo} is the voltage harmonics of point o in Fig. 5b.

$$u_{hMo}=\frac{u_{hMa}+u_{hMb}+u_{hMc}}{3} \tag{6}$$

u_{hMo} can also be expressed as

$$u_{hMo}=\sum_{f=f_{1M}+1}^{\infty} u_{hMfo} \tag{7}$$

The voltage across Z_M of phase a is

$$\Delta u_{hMa}=u_{hMa}-u_{hMo}=u_{hMa}-\frac{u_{hMa}+u_{hMb}+u_{hMc}}{3} \tag{8}$$

According to (3) and (8), Δu_{hMa} can be expressed as

$$\begin{aligned} \Delta u_{hMa} = & u_{hMa}-u_{hMn} \\ = & \sum_{m=1}^{\infty}\Big[A_{m0}\cos(m(\omega_c t+\varphi_{PWMM})) \\ & + B_{m0}\sin(m(\omega_c t+\varphi_{PWMM}))\Big] \\ & + \sum_{m=1}^{\infty}\sum_{\substack{n=-\infty \\ (n\neq 0)}}^{\infty}\Big[A_{mn}\cos(m(\omega_c t+\varphi_{PWMM}) \\ & + n(\omega_0 t+\theta_s+\theta_0)) + B_{mn}\sin(m(\omega_c t+\varphi_{PWMM}) \\ & + n(\omega_0 t+\theta_s+\theta_0))\Big] \quad n\neq 3,6,9\ldots \end{aligned} \tag{9}$$

Equation (9) explains that Δu_{hMa} can be calculated from (3). Δu_{hMa} can also be expressed as

Table 2 Outer and inner integral limit for DPWMMIN

i	$y_1(i)$	$y_2(i)$	$x_1(i)$	$x_2(i)$
1	$\frac{2\pi}{3}$	π	0	0
2	0	$\frac{2\pi}{3}$	$-\frac{\sqrt{3}\pi}{2}D\cos\left(y-\frac{\pi}{6}\right)$	$\frac{\sqrt{3}\pi}{2}D\cos\left(y-\frac{\pi}{6}\right)$
3	$-\frac{2\pi}{3}$	0	$-\frac{\sqrt{3}\pi}{2}D\cos\left(y+\frac{\pi}{6}\right)$	$\frac{\sqrt{3}\pi}{2}D\cos\left(y+\frac{\pi}{6}\right)$
4	$-\pi$	$-\frac{2\pi}{3}$	0	0

Table 3 Example of the look-up table

D	1	2	3	4	5	6	7	8	9	10
0.01	C_{10}	C_{11}	C_{12}	C_{14}	C_{15}	C_{20}	C_{21}	C_{22}	C_{24}	C_{25}
⋮	⋮	⋮	⋮	⋮	⋮	⋮	⋮	⋮	⋮	⋮
1.15	C_{10}	C_{11}	C_{12}	C_{14}	C_{15}	C_{20}	C_{21}	C_{22}	C_{24}	C_{25}

$$\Delta u_{\mathrm{h}M\mathrm{a}} = \sum_{f=f_{1M}+1}^{\infty} \Delta u_{\mathrm{h}Mf\mathrm{a}} \tag{10}$$

It is impractical to calculate all harmonics in (9), so only the dominant high frequency harmonics are taken into consideration. In this paper, only harmonics with following multiple indices and fundamental multiple indices are involved in calculation: $m = 1$ $(n = 0,1,2,4,5)$, $m = 2$ $(n = 0,1,2,4,5)$. Even so, it still costs much time to calculate A_{mn} and B_{mn}. For easily calculating the current harmonics, C_{mn} can be defined as (11), which is a complex value.

$$\begin{cases} C_{mn} = \dfrac{A_{mn} + \mathrm{j}B_{mn}}{V_{\mathrm{dc}}} \\ A_{mn} + \mathrm{j}B_{mn} = C_{mn}V_{\mathrm{dc}} \end{cases} \tag{11}$$

Since A_{mn} and B_{mn} are the functions of modulation index D and V_{dc}, the look-up table method can be employed to calculate C_{mn} according to D. Then, A_{mn} and B_{mn} can be calculated with C_{mn} and V_{dc}. D ranges from 0 to 1.15 for DPWMMIN. The step resolution of D is 0.01 in the look-up table. So, the size of the table is 115 × 10. Table 3 shows an example of the look-up table. Then, $\Delta u_{\mathrm{h}Mf\mathrm{a}}$ can be calculated according to C_{mn} in the look-up table. The look-up tables of other modulation methods can also be developed by using the above method.

4.2 Calculation of current harmonics

Figure 5c shows the equivalent circuit for harmonic with frequency f, where the phasor can be employed to calculate the harmonic current with the specific frequency f of phase a in inverter M:

$$\dot{I}_{\mathrm{h}Mf\mathrm{a}} = \frac{\Delta \dot{U}_{\mathrm{h}Mf\mathrm{a}}}{Z_{Mf}} \tag{12}$$

Then, the total current harmonic with frequency f can be derived as:

$$\begin{aligned} \dot{I}_{\mathrm{hsum}f\mathrm{a}} &= I_{\mathrm{hsum}f\mathrm{a}} \exp(\mathrm{j}\varphi_{\mathrm{hsum}f\mathrm{a}}) = \sum_{M=1}^{N} I_{\mathrm{h}Mf\mathrm{a}} \exp(\mathrm{j}\varphi_{i\mathrm{h}Mf\mathrm{a}}) \\ &= \sum_{M=1}^{N} I_{\mathrm{h}Mf\mathrm{a}} \exp(\mathrm{j}\Phi_{i\mathrm{h}Mf\mathrm{a}}(\varphi_{\mathrm{PWM}M})) \\ &= W_f(\varphi_{\mathrm{PWM1}}, \varphi_{\mathrm{PWM2}}, \ldots, \varphi_{\mathrm{PWM}N}) \end{aligned} \tag{13}$$

The amplitude and phase angle are

$$I_{\mathrm{hsum}f\mathrm{a}} = \left|W_f\right| = W_{1f}(\varphi_{\mathrm{PWM1}}, \varphi_{\mathrm{PWM2}}, \ldots, \varphi_{\mathrm{PWM}N}) \tag{14}$$

$$\varphi_{\mathrm{hsum}f\mathrm{a}} = \mathrm{angle}(W_f) = W_{2f}(\varphi_{\mathrm{PWM1}}, \varphi_{\mathrm{PWM2}}, \ldots, \varphi_{\mathrm{PWM}N}) \tag{15}$$

where W_f, W_{1f} and W_{2f} are functions of $\varphi_{\mathrm{PWM}M}$.

The purpose of this section is to get the relationship between phase shift angle of $\varphi_{\mathrm{PWM}M}$ and the total harmonic current of phase a:

$$I_{\mathrm{hsum}\mathrm{a}} = \sqrt{\sum_{f=f_{1M}+1}^{\infty} I_{\mathrm{hsum}f\mathrm{a}}^2} = F(\varphi_{\mathrm{PWM1}}, \varphi_{\mathrm{PWM2}}, \ldots, \varphi_{\mathrm{PWM}N}) \tag{16}$$

where F is the function of $\varphi_{\mathrm{PWM}M}$.

So, the THD of total current is

$$H_{\mathrm{suma}} = \sqrt{\frac{I_{\mathrm{hsuma}}^2}{I_{1\mathrm{suma}}^2}} \tag{17}$$

where $I_{1\mathrm{suma}}$ is the root mean square (RMS) value of total fundamental current of phase a, which can be written as

$$I_{1\mathrm{suma}} = \sqrt{\sum_{M=1}^{N} I_{1M\mathrm{a}}^2} \tag{18}$$

where $I_{1M\mathrm{a}}$ is the RMS value of output fundamental current of inverter M.

5 Fast intelligent method to calculate $\varphi_{\mathrm{PWM}M\mathrm{best}}$ and f_{synmin}

Reference [19] has proposed a PSO method to calculate $\varphi_{\mathrm{PWM}M\mathrm{best}}$ and f_{synmin}. But it costs too much time because the initial positions of particles are random. Given that the DC-link voltage and power factor of distributed inverters will not change rapidly, the difference between two adjacent calculation results is almost invariable. This section therefore proposes a fast intelligent method to calculate $\varphi_{\mathrm{PWM}M\mathrm{best}}$ and f_{synmin}. In detail, when calculating $\varphi_{\mathrm{PWM}M\mathrm{best}}$ in every iteration process, the initial position of each particle is set as $\varphi_{\mathrm{PWM}M\mathrm{best}}$ of the last iteration. But when calculating f_{synmin} at the first iteration process, the intermediate calculation results of $\varphi_{\mathrm{PWM}M\mathrm{best}}$ can be employed to choose the initial value of f_{synmin} unlike that in [19], and then the initial f_{syn} during every iteration is set as the obtained value of the last calculation. Doing so, the calculation speed can be improved up to 5 to 10 times due to the first initial value of f_{syn} is not far from the final result of f_{synmin}.

5.1 Calculation of $\varphi_{\mathrm{PWM}M\mathrm{best}}$

To calculate $\varphi_{\mathrm{PWM}M\mathrm{best}}$, Eq. (16) should be minimized as (19), which is actually an optimization problem.

$$\begin{cases} \min & I_{\mathrm{hsuma}} = F(\varphi_{\mathrm{PWM1}}, \varphi_{\mathrm{PWM2}}, \ldots, \varphi_{\mathrm{PWMN}}) \\ \text{s.t.} & 0^\circ < \varphi_{\mathrm{PWMM}} < 360^\circ \quad M = 1, 2, \ldots, N \end{cases} \tag{19}$$

This paper adopts the PSO method [21, 22] to solve (19). Specifically, the optimization method should initialize the position and the velocity of each particle and then find the optimal phase shift angle. Two parts of calculating $\varphi_{\mathrm{PWM}M\mathrm{best}}$ are elaborated in the following.

5.1.1 Part A

For the first calculation of $\varphi_{\mathrm{PWM}M\mathrm{best}}$, the initial position and the velocity of particle x are defined as $\boldsymbol{\varphi}_x(0)$ and $\boldsymbol{v}_x(0)$ ($x = 1, 2, \ldots, X_{\max}$), respectively. $\boldsymbol{\varphi}_x(0)$ and $\boldsymbol{v}_x(0)$ could be derived as (20) and (21), respectively.

$$\begin{cases} \boldsymbol{\varphi}_x(0) = [\varphi_{\mathrm{PWM1}x}(0), \varphi_{\mathrm{PWM2}x}(0), \ldots, \varphi_{\mathrm{PWM}N x}(0)] \\ \varphi_{\mathrm{PWM1}x}(0) = 0 \\ \varphi_{\mathrm{PWM}M x}(0) = \mathrm{rand}([0^\circ, 360^\circ]) \quad M = 2, 3, \ldots, N \end{cases} \tag{20}$$

$$\begin{cases} \boldsymbol{v}_x(0) = [v_{\mathrm{PWM1}x}(0), v_{\mathrm{PWM2}x}(0), \ldots, v_{\mathrm{PWM}N x}(0)] \\ v_{\mathrm{PWM1}x}(0) = 0 \\ v_{\mathrm{PWM}M x}(0) = v_{\max}\mathrm{rand}([-1, 1]) \quad M = 2, 3, \ldots, N \end{cases} \tag{21}$$

After the first calculation of $\varphi_{\mathrm{PWM}M\mathrm{best}}$, the initial velocity is still expressed with (21). But the initial position of particle x will employ the result of the last calculation:

$$\boldsymbol{\varphi}_x(0) = [\varphi_{\mathrm{PWM1best}}, \varphi_{\mathrm{PWM2best}}, \ldots, \varphi_{\mathrm{PWM}N\mathrm{best}}] \tag{22}$$

5.1.2 Part B

During the calculation, the PSO method should first initialize c as 0 and then calculate the I_{hsumax} of each particle by using (23).

$$I_{\mathrm{hsumax}}(c) = F(\boldsymbol{\varphi}_{\boldsymbol{x}}(c)) \quad x = 1, 2, \ldots, X_{\max} \tag{23}$$

After one iteration, the GSU should save the historical best position of particle x as $\boldsymbol{\varphi}_{x\mathrm{best}}$, and save the historical best positions of all particles as $\boldsymbol{\varphi}_{\mathrm{gbest}}$. Then PSO method increases c by 1 and updates the position and the velocity of particle x by using the method presented in Part A:

$$\begin{cases} \boldsymbol{v}_x(c) = \{\boldsymbol{v}_x(c-1) + a_1\ \mathrm{rand}_1([0, 1])[\boldsymbol{\varphi}_{x\mathrm{best}} - \boldsymbol{\varphi}_x(c-1)] \\ \qquad\quad + a_2\ \mathrm{rand}_2([0, 1])[\boldsymbol{\varphi}_{\mathrm{gbest}} - \boldsymbol{\varphi}_x(c-1)]\} \\ \boldsymbol{\varphi}_x(c) = \boldsymbol{\varphi}_x(c-1) + \boldsymbol{v}_x(c) \end{cases} \tag{24}$$

The PSO method will repeat the above calculation method until $c > c_{\max}$, where $c_{\max}$ is the max iteration times.

Finally, the PSO method could find the optimal phase shift angle of $\boldsymbol{\varphi}_{\mathrm{gbest}}$.

$$\boldsymbol{\varphi}_{\mathrm{gbest}}(0) = [\varphi_{\mathrm{PWM1best}}, \varphi_{\mathrm{PWM2best}}, \ldots, \varphi_{\mathrm{PWM}N\mathrm{best}}] \tag{25}$$

5.2 Calculation of f_{synmin}

There are also two main parts to calculate f_{synmin}.

5.2.1 Part A

For the first calculation of f_{synmin}, GSU initializes f_{synmin} by using the following processes.

1) Selecting all the positions whose I_{hsumax} are larger than the allowable THD value H_{allow} in subsection 5.1;
2) Finding the position $\boldsymbol{\varphi}_{\mathrm{bound}}$, which is the nearest one from $\boldsymbol{\varphi}_{\mathrm{gbest}}$ among all the selected positions in process 1) above;
3) Calculating:

$$\Delta\boldsymbol{\varphi}_{\mathrm{bb}} = \left|\boldsymbol{\varphi}_{\mathrm{gbest}} - \boldsymbol{\varphi}_{\mathrm{bound}}\right| = [\Delta\varphi_{\mathrm{bb1}}, \Delta\varphi_{\mathrm{bb2}}, \ldots, \Delta\varphi_{\mathrm{bb}N}] \tag{26}$$

$$\Delta\boldsymbol{\varphi}_{\mathrm{bbmax}} = \max(\Delta\varphi_{\mathrm{bb1}}, \Delta\varphi_{\mathrm{bb2}}, \ldots, \Delta\varphi_{\mathrm{bb}N}) \tag{27}$$

4) Initializing f_{synmin} as

$$f_{\mathrm{synmin}} = \frac{\Delta\varphi_{1\mathrm{s}}}{\Delta\varphi_{\mathrm{bbmax}}} \tag{28}$$

where $\Delta\varphi_{1\mathrm{s}}$ is the maximum deviation of $\varphi_{\mathrm{PWM}M}$ per second.

After the first calculation, GSU will then initialize f_{synmin} as the f_{syn} of the last calculation process during the next iteration.

5.2.2 Part B

With the known f_{synmin}, the maximum THD of total current, $H_{\max}$, at PCC can be calculated by using (29).

$$\begin{cases} \max\ I_{\mathrm{hsumax}} = F(\varphi_{\mathrm{PWM1}}, \varphi_{\mathrm{PWM2}}, \ldots, \varphi_{\mathrm{PWM}N}) \\ \text{s.t.}\quad \varphi_{\mathrm{PWM}M\mathrm{best}} - \Delta\varphi_{M\max} < \varphi_{\mathrm{PWM}M} < \varphi_{\mathrm{PWM}M\mathrm{best}} + \Delta\varphi_{M\max} \\ \qquad\qquad M = 1, 2, \ldots, N \end{cases} \tag{29}$$

where $\Delta\varphi_{M\max}$ is the maximum deviation of $\varphi_{\mathrm{PWM}M}$ between two synchronization signals. When $H_{\max}$ is lower than H_{allow}, f_{synmin} could be treated as the final calculation result. On the other hand, when $H_{\max}$ is higher than H_{allow}, GSU will increase f_{synmin} and recalculate (29). The corresponding flow chart is shown in Fig. 6.

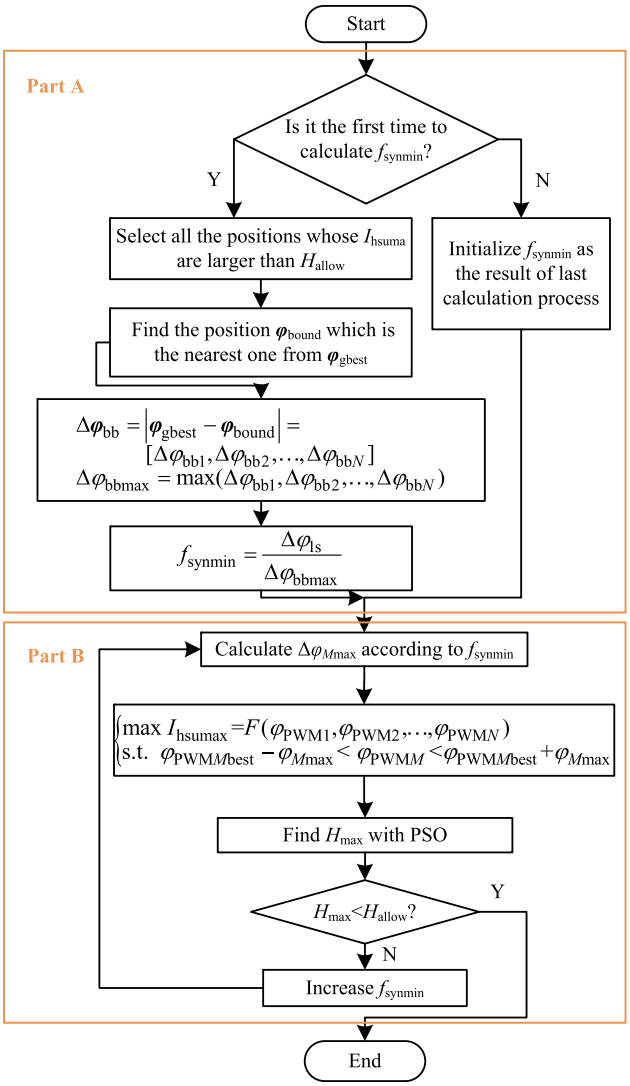

Fig. 6 Flow chart of calculating f_{synmin}

6 Simulation verification

MATLAB/Simulink is used to verify the performance of GSDPWM for three-phase inverters. Firstly, the two inverters with parameters shown in Table 1 are used to verify GSDPWM. f_{syn} is set to be 2 Hz. Figure 7 shows the THD trajectories with or without GSDPWM. The THD of total current will change between the minimum value and the maximum value without GSDPWM. And the THD of total current is obviously lowered down by using GSDPWM. Figure 8a shows the waveforms of total current without GSDPWM. Figure 8b shows the waveform of total current with GSDPWM. Figure 9a, b show the fast Fourier transform (FFT) spectrums of currents in Fig. 8a, b, respectively. It is obvious that the total current has smaller current ripple and its THD is low when GSDPWM is employed.

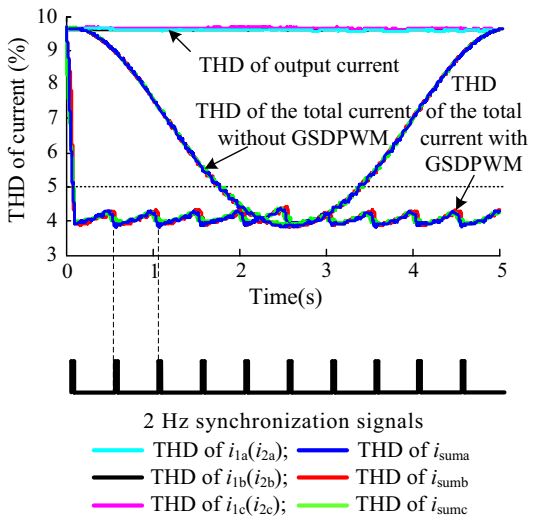

Fig. 7 THD trajectories of the total current and the output currents of two inverters with or without GSDPWM

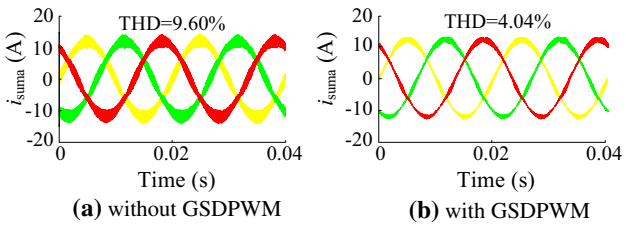

Fig. 8 Simulation waveforms of i_{suma}, i_{sumb} and i_{sumc}

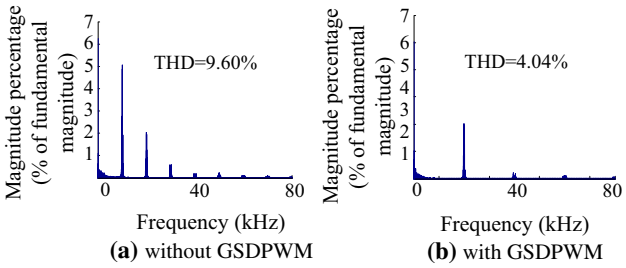

Fig. 9 FFT spectrum of i_{suma}

Next, six inverters with different parameters and different types of DPWM are used to verify the general performance of GSDPWM. The parameters of six inverters are listed in Table 4. When using GSDPWM method to calculate the $\varphi_{PWMMbest}$, the corresponding calculation results are listed in Table 4 too. And the calculation result of f_{synmin} is 20 Hz. Figure 10a shows the THD trajectories of total current with or without GSDPWM, where the THD of i_{suma} changes with time progresses when not adopting GSDPWM. Figure 10b shows the FFT spectrum of i_{suma} at point *A* of Fig. 10a. And the FFT spectrum of i_{suma} when using GSDPWM is shown in Fig. 10c.

Table 4 Parameters of six three-phase inverters

M	U_{dcM} (V)	L_M (mH)	f_{cM} (kHz)	P_M (W)	DPWM type	$\varphi_{PWMMbest}$ (°)
1	700	3.5	10.00006	3	DPWM0	0
2	650	4.5	5.00002	5	DPWM1	216
3	710	4.5	4.99993	4.2	DPWM2	126
4	680	3.5	9.9999	2.8	DPWM3	252
5	705	4.3	4.99992	4	DPWMMAX	36
6	670	3.7	9.99996	2.6	DPWMMIN	72

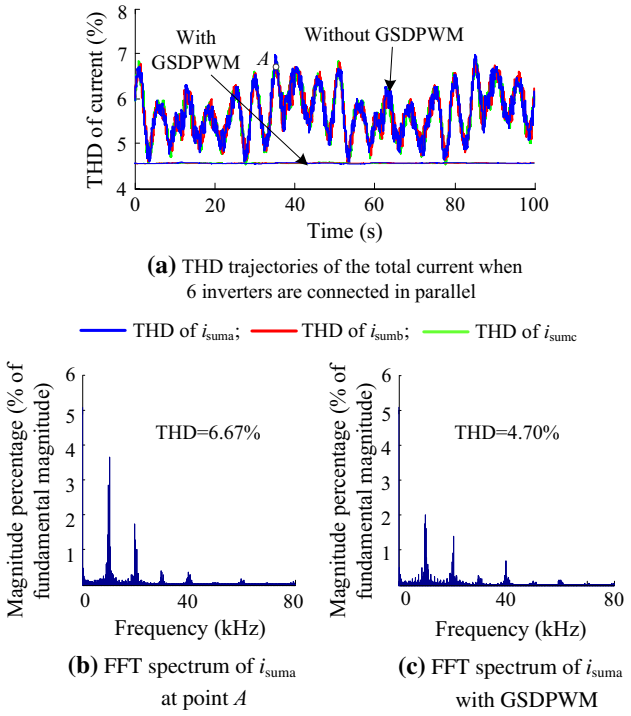

(a) THD trajectories of the total current when 6 inverters are connected in parallel

(b) FFT spectrum of i_{suma} at point A

(c) FFT spectrum of i_{suma} with GSDPWM

Fig. 10 Simulation results of 6 inverters with or without GSDPWM

In [19], the initial value of f_{synmin} in the first iteration process is set as the maximum frequency of communication. Considering that the synchronization frequency cannot be higher than the switching frequency, the initial value is 5 kHz, which is far from the final result 20 Hz. When employing the fast intelligent method, $\boldsymbol{\varphi}_{bound}$ is [0°, 210°, 129°, 244°, 31°, 75°]. So $\Delta\boldsymbol{\varphi}_{bb}$ is [0°, 6°, 3°, 8°, 5°, 3°]. $\Delta\varphi_{bbmax} = 8°$. And $f_{synmin} = 72°/8° = 9$ Hz. The initial value of f_{synmin} is close to the final result 20 Hz. So it costs less time to find the final result.

7 Experimental verification

The experimental prototype was constructed by using two three-phase voltage source inverters. Each inverter has its own independent DC source, conversion circuit, first order filter, and digital controller. The parameters of two inverters are listed in Table 5. These two inverters are connected to a programmable AC voltage source AMETEK-CI-4500LS, whose RMS value of phase voltage is 110 V and the output frequency is 50 Hz.

Firstly, two three-phase inverters are connected in parallel without using GSDPWM. Considering that the THD of i_{suma}, i_{sumb} and i_{sumc} are the same under steady-state condition, only i_{suma} was recorded to calculate the THD trajectory. LECROY oscilloscope was used to continuously record 400 waveforms of i_{suma} in 200 s. The length of each waveform is 0.05 s. Then, MATLAB/Simulink was used to calculate the THD of each waveform. Finally, these 400 THD values were drawn in figures. The THD of i_{suma} is shown by the red line in Fig. 11a, which is similar as the simulation result.

Then, GSDPWM is employed and the THD trajectory of i_{suma} is shown by the green line in Fig. 11a, which is almost constant during the operation. Figure 11b shows the experimental waveforms without GSDPWM, and the THD of output current is up to 9.3 %. Figure 11c shows the experimental waveforms with GSDPWM, and the THD of output current is reduced to 4.8 %. In addition, W_a is the PWM sequence signals of the upper IGBT in phase a, and it is discontinuous by adopting the DPWMMIN method. Figure 12a shows the waveforms of W_{1a}, W_{2a} and the synchronization signals. W_{1a} and W_{2a} are the PWM sequence signals of inverter 1 and 2, respectively. The frequency of synchronization signals is 20 Hz. Figure 12b

Table 5 Parameters of two experimental inverters

Inverter	Switchting frequency (kHz)	DC voltage (V)	Filter inductance (mH)	Active power (kW)	DPWM type	IGBT	Utility grid
1	≈10	350	3.5	1	DPWMMIN	Infineon FF100R12RT4	50 Hz/ 110 V
2	≈10	240	3.5	1	DPWMMIN		

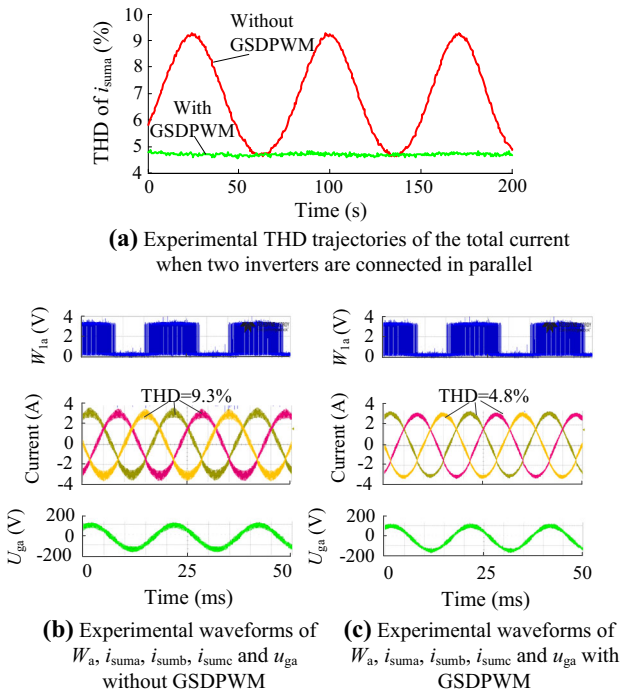

(a) Experimental THD trajectories of the total current when two inverters are connected in parallel

(b) Experimental waveforms of W_a, i_{suma}, i_{sumb}, i_{sumc} and u_{ga} without GSDPWM

(c) Experimental waveforms of W_a, i_{suma}, i_{sumb}, i_{sumc} and u_{ga} with GSDPWM

Fig. 11 Experimental results of two inverters with or without GSDPWM

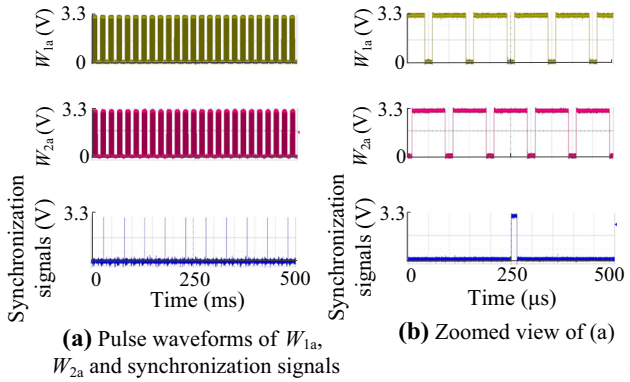

(a) Pulse waveforms of W_{1a}, W_{2a} and synchronization signals

(b) Zoomed view of (a)

Fig. 12 Experimental results of pulse waveforms and synchronization signals

is the zoomed view of Fig. 12a, where the phase shift between W_{1a} and W_{2a} is 180°.

8 Conclusion

This paper proposes a fast global synchronous discontinuous pulse width modulation (GSDPWM) method, which can reduce the total high frequency current harmonics when many inverters with DPWM, third-harmonic PWM and SVPWM are connected to the same PCC. The look-up table method is employed to greatly improve the current harmonic calculation speed. Then, a new fast processing method to calculate the important optimal phase shift angles and the frequency of sending synchronization signals is introduced. GSDPWM can be employed among inverters with different PWM types and parameters. Finally, MATLAB simulation and experimental results verified the performance of GSDPWM.

References

[1] Blaabjerg F, Chen Z, Kjaer SB et al (2004) Power electronics as efficient interface in dispersed power generation systems. IEEE Trans Power Electron 19(5):1184–1194

[2] Blaabjerg F, Teodorescu R, Liserre M et al (2006) Overview of control and grid synchronization for distributed power generationsystems. IEEE Trans Ind Electron 53(5):1398–1409

[3] Xue YS, Chang LC, Kjær SB et al (2004) Topologies of single-phase inverters for small distributed power generators: an overview. IEEE Trans Power Electron 19(5):1305–1314

[4] Ding GQ, Wei R, Zhou K et al (2015) Communication-less harmonic compensation in a multi-bus microgrid through autonomous control of distributed generation grid-interfacing converters. J Mod Power Syst Clean Energy 3(4):597–609. doi:10.1007/s40565-015-0158-3

[5] Ghiani E, Pilo F (2015) Smart inverter operation in distribution networks with high penetration of photovoltaic systems. J Mod Power Syst Clean Energy 3(4):504–511. doi:10.1007/s40565-015-0165-4

[6] Tan GJ, Deng QW, Liu Z (2014) An optimized SVPWM strategy for five-level active NPC (5L-ANPC) converter. IEEE Trans Power Electron 29(1):386–395

[7] Morais LMF, Donoso-Garcia PF, Seleme SI et al (2007) Acoustic resonance avoidance in high pressure sodium lamps via third harmonic injection in a PWM inverter-based electronic ballast. IEEE Trans Power Electron 22(3):912–918

[8] Holmes DG, Lipo TA (2003) Pulse width modulation for power converters: principles and practice. Wiley, New York, pp 241–249

[9] Bhattacharya S, Mascarella D, Joos G (2014) Interleaved SVPWM and DPWM for dual three-phase inverter-PMSM: An automotive application. In: Proceedings of the 2014 IEEE transportation electrification conference and expo (ITEC'14), Dearborn, 6 pp. Accessed 15–18 June 2014

[10] Alexander DR, Williams SM (1993) An optimal PWM algorithm implementation in high performance 125 kVA inverter. In: Proceedings of the 8th annual applied power electronics conference and exposition (APEC'93), San Diego, pp 771–777. Accessed 7–11 Mar 1993

[11] Kolar JW, Ertl H, Zach FC (1991) Influence of the modulation method on the conduction and switching losses of a PWM converter system. IEEE Trans Ind Appl 27(6):1063–1075

[12] Hava AM, Kerkman RJ, Lipo TA (1998) A high-performance generalized discontinuous PWM algorithm. IEEE Trans Ind Appl 34(5):1059–1071

[13] Xing K, Lee FC, Borojevic D et al (1999) Interleaved PWM with discontinuous space-vector modulation. IEEE Trans Power Electron 14(5):906–917
[14] Gabe IJ, Montagner VF, Pinheiro H (2009) Design and implementation of a robust current controller for VSI connected to the grid through an LCL filter. IEEE Trans Power Electron 24(6):1444–1452
[15] Houari A, Renaudineau H, Martin JP et al (2012) Flatness-based control of three-phase inverter with output LC filter. IEEE Trans Ind Electron 59(7):2890–2897
[16] Ding GQ, Gao F, Tang Y, et al (2014) A novel harmonic control approach of distributed generation converters in a weak microgrid. In: Proceedings of the 29th annual IEEE applied power electronics conference and exposition (APEC'14), Fort Worth, pp 2132–2139. Accessed 16–20 Mar 2014
[17] Agorreta JL, Borrega M, López J et al (2011) Modelling and control of *N*-paralleled grid-connected inverters with LCL filter coupled due to grid impedance in PV plants. IEEE Trans Power Electron 26(3):770–785
[18] Abusara MA, Sharkh SM (2013) Design and control of a grid-connected interleaved inverter. IEEE Trans Power Electron 28(2):748–764
[19] Xu T, Gao F, Wei R (2015) Global synchronous pulse width modulation of distributed inverters. In: Proceedings of the 9th international conference on power electronics and ECCE Asia (ICPE-ECCE Asia'15), Seoul, pp 1252–1259. Accessed 1–5 June 2015
[20] Xu T, Gao F, Duan W et al (2015) Performance analysis of global synchronous pulsewidth modulation for distributed inverters. In: Proceedings of the 2015 IEEE energy conversion congress and exposition (ECCE'15), Montreal, pp 6475–6482. Accessed 20–24 Sept 2015
[21] Kennedy J, Eberhart R (1995) Particle swarm optimization. In: Proceedings of the IEEE international conference on neural networks, vol 4, Perth, pp 1942–1948. Accessed 27 Nov–1 Dec 1995
[22] Eberhart R, Kennedy J (1995) A new optimizer using particle swarm theory. In: Proceedings of the 6th international symposium on micro machine and human science (MHS'95), Nagoya, pp 39–43. Accessed 4–6 Oct 1995

Tao XU received B. Eng. degree in electrical engineering from Shandong University, Jinan, China, in 2014. He is currently working toward the Ph.D. degree at the School of Electrical Engineering, Shandong University, Jinan, China. His research interests include power quality, DC/AC microgrid.

Ran WEI received the B. Eng. and M. Eng. degrees in electrical engineering from Shandong University, Jinan, China, in 2002 and 2005, respectively. He is currently working in State Grid Jining Electric Power Supply Company, Jining, China. His research interests include power grid dispatching operation and relay protection.

Ke ZHOU graduated from Harbin Institute of Technology, Harbin, China, in 2003. He is currently working in State Grid Jining Electric Power Supply Company, Jining, China. His research interests include the control of distributed power generation.

Feng GAO (S'07-M'09) received the B. Eng. and M. Eng. degrees in electrical engineering from Shandong University, Jinan, China, in 2002 and 2005, respectively, and the Ph.D. degree from the School of Electrical and Electronic Engineering, Nanyang Technological University, Singapore, in 2009. From 2008 to 2009, he was a research fellow in Nanyang Technological University. Since 2010, he joined the School of Electrical Engineering, Shandong University, where he is currently a professor and serving as Vice Dean. From September 2006 to February 2007, he was a visiting scholar at the Institute of Energy Technology, Aalborg University, Aalborg, Denmark. Dr. Gao was the recipient of the IEEE Industry Applications Society Industrial Power Converter Committee Prize for a paper published in 2006, and he is now serving as an Associate Editor of the IEEE TRANSACTIONS ON POWER ELECTRONICS.